Arq. Bras. Med. Vet. Zootec., v.78, n.3, e13655, 2026

http://dx.doi.org/10.1590/1678-4162-13655
Communication - Veterinary Medicine

Communication

[*Comunicação*]

Pulmonary and abdominal imaging in a FeLV-positive cat with disseminated infection by *Cryptococcus gatti* species complex

[*Imagens pulmonares e abdominais de um gato positivo para FeLV com infecção disseminada pelo complexo de espécies Cryptococcus gatti*]

J.N.P. *Castro*[1], M.W. *Magnabosco*[1], S.B. *Waller*[2], A.R. *Gomes*[2], R.O. *de Faria*[2], G.A.O. *Cavalcanti*[3], P.P.C. *Costa*[3,*]

[1]Graduação, Faculdade de Veterinária, Universidade Federal de Pelotas, UFPEL, Pelotas, RS, Brasil
[2]Centro de Diagnóstico e Pesquisa em Micologia Veterinária (MicVet), Departamento de Doenças Infecciosas, Faculdade de Veterinária, UFPEL, Pelotas, RS, Brasil
[3]Departamento de Clínicas Veterinárias, Faculdade de Veterinária, UFPEL, Pelotas, RS, Brasil

Cryptococcosis is a systemic mycosis caused by fungi of the *Cryptococcus* genus, with *C. neoformans* and *C. gattii* being the main species of clinical relevance in felines (Brito-Santos *et al*., 2019; Reis *et al*., 2021), which are clinically indistinguishable (Ye *et al*., 2025). The infection primarily occurs through the inhalation of environmental yeasts present in contaminated environments, leading to colonization of the respiratory tract and possible dissemination to other organs (Reis *et al*., 2021). Clinical signs vary depending on the affected organ, with cutaneous and neurological forms being the most frequently reported presentations. These can manifest as lymphadenopathy, lethargy, anorexia, chronic nasal discharge, and progressive neurological signs (Huang *et al*., 2023; Russell *et al*., 2025; Choi *et al*., 2025; Tóth *et al*., 2025).

Although immunocompromised cats, such as those positive for feline leukemia virus (FeLV) and feline immunodeficiency virus (FIV), may present with more severe infections (Wronski *et al*., 2023), cryptococcosis can also affect immunocompetent felines (Ballard *et al*., 2025). *Cryptococcus* spp. infection primarily occurs through the inhalation of spores, with initial colonization in the nasal cavity (Wong *et al*., 2024), and possible dissemination to the lungs and other organs, such as the CNS (Huang *et al*., 2023) and abdominal involvement (Johnson *et al*., 2021; Teh *et al*., 2024), especially in immunocompromised individuals.
Computed tomography is a valuable tool for diagnosing pulmonary cryptococcosis in felines, providing detailed images of internal structures (Schlacks *et al*., 2021). However, its availability is limited in many veterinary clinics due to high costs and the need for specialized equipment. In this context, thoracic radiography emerges as an accessible and effective diagnostic alternative. Radiographs can reveal pulmonary changes indicative of cryptococcosis, facilitating early detection and appropriate management. Therefore, it is essential for veterinary professionals to leverage thoracic radiography in identifying suspected cases of pulmonary cryptococcosis, ensuring timely diagnosis and treatment for affected cats.

Among the species that cause cryptococcosis, the infections by the members of the *C. gattii* complex have been increasingly recognized in animals, especially in dogs and cats (Ballard *et al*., 2025). However, the clinical and epidemiological aspects of this infection in veterinary medicine remain poorly explored.

In this study, we present the thoracic radiographic findings of a Siamese cat, FeLV-positive, previously diagnosed with cryptococcosis (Costa *et al*., 2022), in which the fungal agent was molecularly identified as belonging to the *C. gattii* species complex. This

*Corresponding author: paulapriscilamv@yahoo.com.br
Submitted: July 21, 2025. Accepted: January 22, 2026.

approach complements the characterization of the disease, emphasizing the importance of imaging in the early recognition of pulmonary cryptococcosis in felines and the molecular relevance for accurate diagnosis. The case presented expands the knowledge of systemic infection by the *C. gattii* species complex in an immunosuppressed patient (FeLV-positive), highlighting pulmonary involvement, supported by a thorough radiographic evaluation.

A six-year-old neutered male Siamese cat, FeLV-positive, was referred to the diagnostic imaging department of the Veterinary Clinic of Federal University of Pelotas (UFPEL, Pelotas/RS). The cat had a history of left-sided mandibular lymphadenopathy, anorexia, and lethargy. Fine-needle aspiration (FNA) cytology of the lymph node revealed oval encapsulated structures, suggestive of *Cryptococcus* spp., being previously published (Costa *et al.*, 2022). Blood tests, including a complete blood count and biochemical profile (ALT, creatinine, urea, and alkaline phosphatase), were within normal limits for the species. Given the clinical signs of *Cryptococcus* spp. involvement in the systemic organs, the patient underwent detailed imaging, including thoracic radiography, full abdominal ultrasound, and mycological examination.

On radiographic examination, the right and left lateral (LL) and ventrodorsal thoracic projections were evaluated, revealing diffuse moderate bronchoalveolar pulmonary opacification and the presence of an esophageal tube (Fig. 1). Ultrasound examination revealed a heterogeneous hyperechoic formation (Fig. 2A) located cranial to the urinary bladder (Fig. 2B) with a cavitary structure containing hypoechoic fluid and amorphous hyperechoic material in sedimentation. The structure measured approximately 9.46 cm in length and 3.52cm in height, displaying vascularization in its solid portion on Power Doppler evaluation (Fig. 2C). Bilateral hyperechoic nephromegaly with heterogeneous echotexture and hyperechoic areas at the renal caudal poles, along with partial loss of corticomedullary differentiation, were noted (Fig. 2D). Additionally, enlargement of the medial iliac (Fig. 2E) and jejunal lymph nodes (Fig. 2F) was observed.

A direct examination using India ink staining (Acrilex, São Bernardo do Campo, São Paulo, Brazil) revealed large yeast cells with prominent capsules. Upon culturing, no growth was observed on the mycelial agar. However, cream-colored, smooth, mucoid, yeast-like colonies were observed on Sabouraud Dextrose Agar (SDA) incubated at 37°C. When inoculated on Niger seed agar (caffeic acid agar), the colonies turned brown, indicating melanin production. Furthermore, on Canavanine Glycine Bromothymol Blue (CGB) agar, the medium turned blue within 2–5 days, indicating a biochemical profile compatible with *Cryptococcus gattii*, which was subsequently confirmed by molecular analysis.

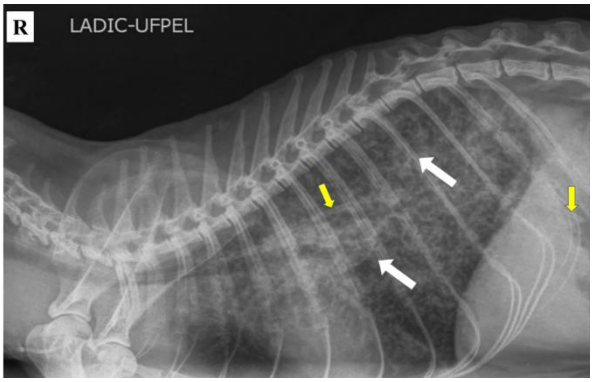

Figure 1. Radiographic image in right (R) lateral projection of a cat with systemic cryptococcosis: diffuse bronchoalveolar pulmonary opacification prominently in the caudal lung lobes (white arrows) and an esophageal tube (yellow arrows) extending from the cervical region to the 12th intercostal space.

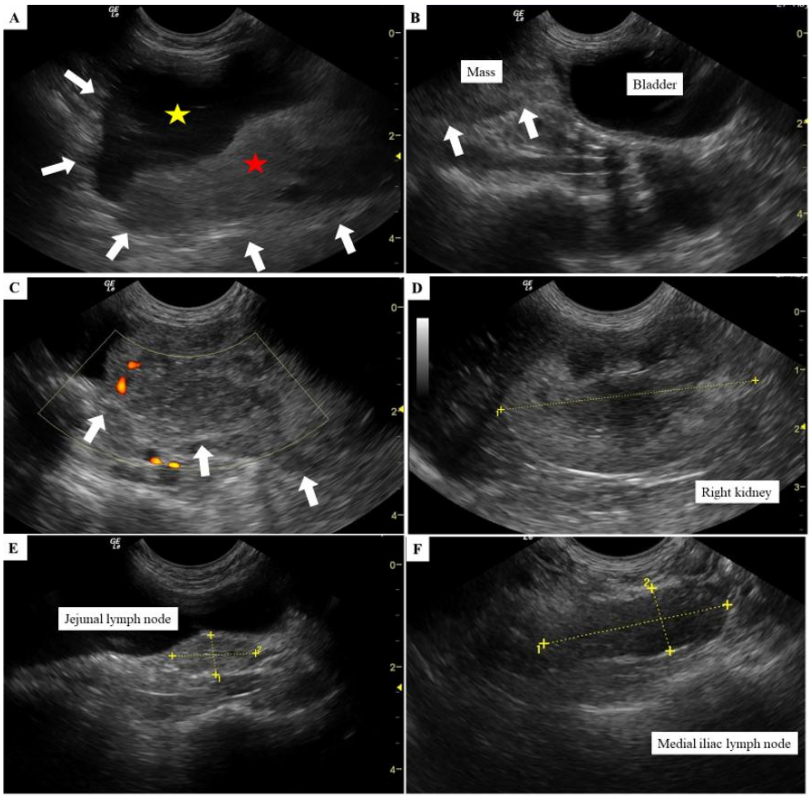

Figure 2. Ultrasonography of the urinary bladder (A-C), right kidney (D), and jejunal (E) and medial iliac (F) lymph nodes in a cat with systemic cryptococcosis. Urinary bladder showing a heterogeneous hyperechoic cavitary formation (arrows in A and B) in B-mode. The formation is located cranial to the urinary bladder, with mixed content including hypoechoic (yellow star, A) and amorphous hyperechoic (red star, A) components. The same formation with heterogeneous hypoechoic characteristics is shown with vascularization (arrows, C) as seen on Power Doppler mode. Right kidney exhibiting increased cortical and medullary echogenicity, partial loss of corticomedullary definition, slightly heterogeneous parenchyma, and a hyperechoic area in the caudal cortex (between calipers) in B-mode (D). Enlargement of the jejunal lymph node (3.17cm×1.11cm) in B-mode (between calipers, E) and enlargement of the medial iliac lymph node (1.62cm×0.78cm) in B-mode (between calipers, F) were also noted.

For molecular confirmation, fungal DNA was extracted from *C. gattii* colonies using the Qiagen DNeasy commercial kit (Qiagen Sample & Assay Technologies, Hilden, Germany), following the breakdown of fungal cell walls with liquid nitrogen. The PCR assay was conducted using universal ITS1 (GAACCWGCGGARGGATCA) and ITS2 (GCTGCGTTCTTCATCGATGC) primers, which amplify the ITS1 and ITS2 regions and *5.8S rRNA* gene (White *et al*., 1990). The conventional PCR targeting the complete ITS region (ITS1–5.8S–ITS2) was performed using Taq DNA polymerase in a reaction containing 1× amplification buffer, $MgCl_2$, dNTPs, and forward and reverse primers. The amplification conditions included an initial denaturation at 95°C for 2–3min, followed by 30–35 cycles of denaturation at 95°C for 30 s, annealing at 50–60°C for 30s, and extension at 72°C for 1–2min, with a final extension at 72°C for 10min, according to classical protocols described for ITS amplification (White *et al*., 1990). The positive controls consisted of in-house fungal DNA from reference samples, whereas nuclease-free water (Invitrogen Corp., Carlsbad, CA, USA) was used as the negative control. The PCR products were separated by electrophoresis on a 2% agarose gel prepared in TBE or TAE buffer, subjected to a constant electric current (≈80–120 V) for a sufficient time to allow adequate fragment separation, stained with ethidium bromide, and visualized under ultraviolet light.

The amplified PCR products were purified using the Illustra GFX PCR DNA and Gel Band Purification Kit (GE Healthcare, Little Chalfont, Buckinghamshire, UK) and subjected to direct sequencing using both forward and reverse primers. Multiple sequence alignments were performed using CLUSTAL W (version 1.4) in the MEGA 6.1 software (Tamura *et al*., 2013), followed by the generation of a sequence identity matrix with BioEdit version 7.2 (Hall *et al*., 1999) to identify differences in the nucleotide positions within the ITS1 and ITS2 regions and the *5.8S rRNA* gene of *Cryptococcus* species (Katsu *et al*., 2004). The selected sequences are representative of the ITS and molecular groups within the *C. neoformans* and *C. gattii* species complex.

The PCR assay amplified a 557-bp fragment from the ITS1 and ITS2 regions of the fungal colonies. Direct sequencing confirmed the amplicon to be *C. gattii*. BLAST analysis showed 99–100% sequence identity with *C. gattii* isolates in GenBank. The methodology employed does not allow for differentiation of species within the *C. gatti* complex; therefore, the identification was concluded at the complex level.

The patient was treated orally with compounded fluconazole (18mg every 12 h) for two months, showed clinical improvement (Costa *et al.*, 2022). The animal was in good health at the time of writing this article, although no follow-up examinations were performed because of the owners' decisions.

Radiographic and ultrasonographic studies on cryptococcosis in dogs and cats are limited, and their findings are often unremarkable (Russell *et al*., 2025; Choi *et al*., 2025). However, in the reported patient, thoracic radiographic alterations and abdominal ultrasound findings indicated that the cat presented with a disseminated form of cryptococcosis. FNA has been reported as an efficient diagnostic method for mycosis in companion animals (Brito-Santos *et al*., 2019) and could have confirmed systemic involvement by collecting material from the affected organs, as performed in the patient. It is worth noting that the cervical lymph node aspiration confirmed the presence of *Cryptococcus* sp. (Costa *et al.*, 2022), whose systemic organ involvement is frequently observed (Teh *et al*., 2024; Choi *et al*., 2025).

It is known that feline cryptococcosis does not show any predisposition based on sex or age, and the nasal form is the most common (Russell *et al*., 2025), due to the inhalation of pathogenic fungal propagules. However, there was no history of contact with suspected environmental sources in this case. Although the patient did not display any respiratory signs or upper respiratory tract involvement, thoracic radiography revealed alterations in the pulmonary pattern (Costa *et al.*, 2022), as detailed in this report.

Pulmonary mycoses typically lead to unstructured interstitial pulmonary opacity (diffuse or multifocal), or diffuse alveolar or miliary pulmonary patterns (Schlacks *et al*., 2021). Diffuse mixed alveolar and bronchial pulmonary opacity, which was more pronounced in the caudal lobes, suggested fungal pneumonia. Animals with pulmonary fungal infections generally present with diffuse or multifocal unstructured interstitial pulmonary opacity or an alveolar or nodular pulmonary pattern and less frequently with lymphadenopathy, mediastinal mass, or pleural effusion (Schlacks *et al*., 2021).

Abdominal ultrasonography revealed a complex hyperechoic formation cranial to the bladder. This formation was cavitary with a mixed content of hypoechoic and amorphous hyperechoic material, which can be indicative of mesenteric fungal granuloma. Additionally, bilateral hyperechoic nephromegaly with heterogeneous echotexture was observed, including poorly defined hyperechoic areas in both caudal poles, partial loss of the corticomedullary definition, and slight bilateral pielectasia, suggesting nephropathy. While some animals may exhibit renal involvement without ultrasonographic signs, others may show iso- to hypoechoic nodular renal lesions suggestive of granuloma or pyogranulomatous inflammation, as well as areas of necrosis (Teh *et al*., 2024).

In cases of abdominal cryptococcosis, abdominal ultrasound plays a crucial role in identifying mesenteric and intestinal lesions (Johnson *et al*., 2021). This was also observed in our patient, in which the hyperechoic cavitary formation with heterogeneous content located cranial to the bladder was consistent with a fungal granuloma. The patient also exhibited a mildly thickened gastric wall, suggestive of gastritis, heterogeneous splenomegaly, and jejunal lymphadenopathy.

Splenomegaly, gastrointestinal involvement, and lymphadenopathy are more commonly observed in dogs (Johnson *et al*., 2021), whereas pulmonary involvement is more common in cats (Schlacks *et al*., 2021). The involvement of multiple organs suggests hematogenous dissemination, and systemic signs include lethargy, inappetence, anorexia, and weight loss (Johnson *et al*., 2021), as observed in this case.

However, immunocompetent animals can also be affected by *Cryptococcus* spp. infection (Ballard *et al*., 2025); however, immunocompromised animals are more likely to develop severe forms of cryptococcosis (Wronski *et al*., 2023). The feline patient reported was FeLV-positive, and despite pulmonary involvement evident on imaging studies, the clinical signs were subtle, with lymphadenopathy being the only observed symptom (Costa *et al.*, 2022). Animals with FeLV co-infection experience severe immunosuppression, which can predispose them to or exacerbate systemic infections (Wronski *et al*., 2023). It is believed that the presence of immunosuppressive FeLV in the patient contributed to the severe and disseminated progression of the disease, affecting the pulmonary and urinary systems. Furthermore, animals with cryptococcosis and FeLV positivity often present moderate ocular lesions (Wronski *et al*., 2023).

Ultrasound findings in the patient could be associated with other etiologies such as asthma and bronchial disease (Johnson, 2020; Rozanski, 2016), potentially complicating the diagnosis. In feline asthma, radiographic findings typically show bronchial and bronchointerstitial patterns, and some cases exhibit pulmonary hyperinflation (Trzil, 2020). However, the pulmonary pattern observed in this patient was bronchoalveolar. Generally, feline bronchial disease is characterized by airway thickening with a diffuse bronchial pattern (Ferreira *et al*., 2015), which differs from the pattern observed in the reported patient. Immunocompromised animals may present more severe and disseminated forms of the disease. Therefore, FeLV-positive felines should undergo preventive examinations every six months to detect early changes in their health status.

Oral fluconazole is the recommended antifungal therapy for feline cryptococcosis (Brito-Santos *et al*., 2019), with an excellent response in many cats with advanced or disseminated disease. The use of itraconazole can lead to heteroresistance and, consequently, increase the virulence of *C. gattii* (Ferreira *et al*., 2015). The patient was treated with fluconazole for 2 months, resulting in remission of lymphadenopathy and improved well-being.

This case report highlights that FeLV coinfection exacerbates the dissemination of cryptococcosis, emphasizing the need for imaging studies in FeLV-positive animals suspected to have cryptococcosis. The observed pulmonary and abdominal changes reinforce the systemic nature of infection and the importance of early diagnosis and continuous monitoring.

Keywords: *Cryptococcus gatti* complex species, feline, imaging diagnosis, lymphadenopathy, systemic mycosis

RESUMO

Um gato Siamês de seis anos, castrado e positivo para FeLV, apresentou linfadenopatia mandibular, anorexia e letargia. Os exames de imagem revelaram uma opacificação pulmonar broncoalveolar difusa sugestiva de pneumonia fúngica, formação cavitaria vascularizada próxima à bexiga e nefromegalia bilateral. Cryptococcus gatti *foi identificado por citologia e cultura fúngica, e confirmado por sequenciamento de ITS1-ITS2, classificando o isolado dentro do complexo* C. gatti**,** *embora sem resolução em nível de espécie. O felino foi tratado com fluconazol por dois meses, resultando em melhora clínica. Este caso, previamente relatado por Costa et al. (2022), é retomado aqui com foco em achados radiográficos e ultrassonográficos detalhados e na identificação do complexo* C. gatti. *O relato destaca a grave disseminação sistêmica da criptococose em gatos positivos para FeLV, ressaltando o papel crucial da imagem na detecção precoce e a importância do monitoramento contínuo em pacientes imunocomprometidos para garantir os melhores resultados terapêuticos.*

Palavras-chave: diagnóstico por imagem, espécies do complexo Cryptococcus gatti, *felino, linfadenopatia, micoses sistêmicas*

ACKNOWLEDGMENTS

The authors are grateful to the following Brazilian institutes: to Conselho Nacional de Desenvolvimento Científico e Tecnológico (CNPq), to Coordenação de Aperfeiçoamento de Pessoal de Nível Superior (CAPES), to Fundação de Amparo à Pesquisa do Estado do Rio Grande do Sul (FAPERGS) for student and research scholarships.

ETHICAL ASPECTS

This research was not submitted to the *Ethics Committee on Animal Use*.

CONTRIBUTORS

JNP Castro: clinical management of the case and initial manuscript draft. MW Magnabosco and GAO Cavalcanti: imaging examinations of radiography and ultrasonography. SB Waller: mycological analysis, data interpretation, manuscript drafting, and final version preparation. AR Gomes and RO de Faria: mycological analyses. PPC Costa: clinical management, case design, and contribution to discussion. All authors contributed to study conception, data analysis, discussion, manuscript writing, and approved the final version for publication.

DATA AVAILABILITY STATEMENT

The research data are available upon request.

REFERENCES

BALLARD, S.; MONTGOMERY, A.; ROSE, I. *et al.* Epidemiological study of *Cryptococcus gatti* complex infection in domestic and wild animals in Oregon. *Vet. Sci.*, v.12, p.185, 2025.

BRITO-SANTOS, F.; REIS, R.S.; COELHO, R.A. *et al.* Cryptococcosis due to *Cryptococcus gatti* VGII in southeast Brazil: the one health approach revealing a possible role for domestic cats. *Med. Mycol. Case Rep.*, v.24, p.61-64, 2019.

CHOI, C.H.; KIM, K.; JE, C.Y. *et al.* Rare case of systemic cryptococcal lymphadenopathy in a Persian cat. *Vet. Med. Sci*., v.11, p.e70564, 2025.

COSTA, P.P.C.; WALLER, S.B.; CONTE, C. *et al*. Cryptococcosis by *Cryptococcus* sp. causing lymphadenomegaly as a single sign in a cat. *Mycopathologia*, v.187, p.627-630, 2022.

FERREIRA, G.F.; SANTOS, J.R.A.; COSTA, M.C. *et al.* Heteroresistance to itraconazole alters the morphology and increases the virulence of *Cryptococcus gattii*. *Antimicrob. Agents Chemother.*, v.59, p.4600-4609, 2015.

HALL, T.A. BioEdit: a user-friendly biological sequence alignment editor and analysis program for Windows 95/98/NT. *Nucleic Acids Symp.*, v.41, p.95-98, 1999.

HUANG, C.H.; CHEN, K.S.; CHIA, M.Y. Cryptococcal granulomas of basal ganglia due to *Cryptococcus neoformans* in a cat: a case report and literature review. *J. Vet. Med. Sci.*, v.85, p.412-416, 2023.

JOHNSON L.; MACKAY, B.; KROCKENBERGER, M.B. *et al.* Abdominal cryptococcosis in dogs and cats: 38 cases (2000-2018). *J. Small Anim. Pract.*, v.62, p.19-27, 2021.

JOHNSON, L.R. Diseases of airways. In*:* _____. *Canine and feline respiratory medicine*. 2.ed. [New Jersey]: Wiley-Blackwell, 2020.

KATSU, M.; KIDD, S.; ANDO, A. *et al.* The internal transcribed spacers and 5.8S *rRNA* gene show, extensive diversity among isolates of the *Cryptococcus neoformans* species complex. *FEMS Yeast Res.*, v.4, p.377-388, 2004.

KLEIN, K.R.; HALL, L.; DEML, S.M. *et al.* Identification of *Cryptococcus gattii* by use of L-canavanine glycine bromothymol blue medium and DNA sequencing. *J. Clin. Microbiol.*, v.47, p.3669-3672, 2009.

REIS, R.S.; BONNA, I.C.F.; ANTONIO, I.M.S. *et al. Cryptococcus neoformans* VNII as the main cause of cryptococcosis in domestic cats from Rio de Janeiro, Brazil. *J. Fungi.*, v.7, p.980, 2021.

ROZANSKI, E. Feline lower airway disease. August's consultations. *Feline Intern. Med.*, v.7, p.447-451, 2016.

RUSSELL, O.L.; JOHNSON, D.; ALLAN, F. *et al.* Fungal rhinosinusitis in cats in the United Kingdom: 34 cases (2013-2022). *J. Vet. Intern. Med*., v.39, p.e70076, 2025.

SCHLACKS, S.; BOOZER, T.; DIAL, S. *et al.* CT identifies pulmonary cryptococcosis in a domestic feline. *Vet. Radiol. Ultrasound*, v.62, p.e54-e57, 2021.

TAMURA, K.; STECHER, G.; PETERSON, D. *et al.* MEGA6: molecular evolutionary genetics analysis, version 6.0. *Mol. Biol. Evol.*, v.30, p.725-2729, 2013.

TEH, A.; PRITCHARD, E.; DONAHO, S.L. *et al.* A case of disseminated cryptococcosis with abdominal involvement due to *Cryptococcus neoformans* species complex in a Ragdoll cat and false-negative cryptococcal antigen lateral flow tests due to the postzone phenomenon. *Aust. Vet. J.*, v.102, p.306-312, 2024.

TÓTH, Z.; MÁRIALIGETI, M.; LAJOS, Z. *et al.* Report of a feline *Cryptococcus neoformans* infection in Hungary. *Acta Vet. Hung*., v.73, p.237-242, 2025.

TRZIL, J.E. Feline asthma. *Vet. Clin. North Am. Small Anim. Pract.*, v.50, p.375-391, 2020.

WHITE, T.; BRUNS, T.; LEE, S.J.T. Amplification and direct sequencing of fungal ribosomal RNA genes for phylogenetics. In: INNIS, M.; GELFAND, D.; SNINSKY, J. WHITE, T. *PCR protocols: a guide to methods and applications*. San Diego: Academic Press. 1990, p.315-322.

WONG, S.A.; JACOBSON, E.; PODADERA, J. *et al.* Computed tomography findings of nasal cryptococcosis in Australia (2008-2020): 12 dogs and 9 cats. *Am. J. Vet. Res.*, v.85, n.8, 2024.

WRONSKI, J.G.; CECCO, B.S.; RAITER, J. *et al*. Ophthalmic and immunopathological characterization of systemic infectious diseases in cats. *Vet. Pathol*., v.60, p.352-359, 2023.

YE, W.M.; ZHENG, X.Q.; ZHONG, Y. *et al.* Development of a multiplex qPCR to detect and identify *Cryptococcus neoformans* and *Cryptococcus gattii*. *ACS Omega*, v.10, p.61011-61019, 2025.

Editor-chefe: Marcelo Resende de Souza
Editor-científico: Antônio de Pinho Marques Jr.